

# On the bilateral preconditioning for an L2-type all-at-once system arising from time-space fractional Bloch-Torrey equations

Yong-Liang Zhao<sup>a</sup>, Xian-Ming Gu<sup>b,\*</sup>, Hu Li<sup>c,\*</sup>

<sup>a</sup>*School of Mathematical Sciences, Sichuan Normal University, Chengdu, Sichuan 610068, P.R. China*

<sup>b</sup>*School of Economic Mathematics,*

*Southwestern University of Finance and Economics, Chengdu, Sichuan 611130, P.R. China*

<sup>c</sup>*School of Mathematics, Chengdu Normal University, Chengdu, Sichuan 611130, P.R. China*

---

## Abstract

Time-space fractional Bloch-Torrey equations (TSFBTEs) are developed by some researchers to investigate the relationship between diffusion and fractional-order dynamics. In this paper, we first propose a second-order implicit difference scheme for TSFBTEs by employing the recently proposed L2-type formula [A. A. Alikhanov, C. Huang, Appl. Math. Comput. (2021) 126545]. Then, we prove the stability and the convergence of the proposed scheme. Based on such a numerical scheme, an L2-type all-at-once system is derived. In order to solve this system in a parallel-in-time pattern, a bilateral preconditioning technique is designed to accelerate the convergence of Krylov subspace solvers according to the special structure of the coefficient matrix of the system. We theoretically show that the condition number of the preconditioned matrix is uniformly bounded by a constant for the time fractional order  $\alpha \in (0, 0.3624)$ . Numerical results are reported to show the efficiency of our method.

*Keywords:* Preconditioning, All-at-once system, Toeplitz matrix, Parallel-in-time, L2-type difference scheme

---

## 1. Introduction

Fractional calculus as a generalization of integer calculus fails to attract much attention until the past decades. Due to the hereditary and memory properties of fractional derivatives, fractional differential equations have been successfully used in various fields such as electrical spectroscopy impedance [1, 2], earth system dynamics [3], solute transport in porous media [4] and image processing [5, 6].

In physics, the diffusion model is one of important models for describing the transport process. The particles distributed in a normal bell-shaped pattern based on the Brownian motion are usually described by the classical diffusion model. However, it cannot model the transport process of diffusing particles in a

---

\*Corresponding authors

*Email addresses:* ylzhaofde@sina.com (Yong-Liang Zhao), guxianming@live.cn (Xian-Ming Gu), lihu\_0826@163.com (Hu Li)

fractal media with locally inhomogeneous. The reason could be that this kind of process may no longer obey the classical Fick's law. Recently, numerous experiments show that fractional diffusion equations are more adequate than the classical one to describe anomalous diffusion [7–9]. Particularly, time-space fractional diffusion equations are generally used for modeling the anomalous diffusion, that is, the subdiffusion in time and the super-diffusion in space simultaneously [10]. In this paper, we consider the following time-space fractional Bloch-Torrey equation (TSFBTE) [11, 12]:

$$\begin{cases} {}_0^C \mathcal{D}_t^\alpha u(x, t) = \kappa \frac{\partial^\beta u(x, t)}{\partial |x|^\beta} + f(x, t), & x \in (x_L, x_R), t \in (0, T], \\ u(x_L, t) = u(x_R, t) = 0, & t \in [0, T], \\ u(x, 0) = \phi(x), & x \in (x_L, x_R), \end{cases} \quad (1.1)$$

where  $0 < \alpha \leq 1$ ,  $1 < \beta \leq 2$ , the diffusion coefficient  $\kappa > 0$ ,  $\phi(x)$  and  $f(x, t)$  are given functions. In Eq. (1.1),  ${}_0^C \mathcal{D}_t^\alpha u(x, t)$  and  $\frac{\partial^\beta u(x, t)}{\partial |x|^\beta}$  are the Caputo and the Riesz fractional derivatives [13] defined as follows:

$${}_0^C \mathcal{D}_t^\alpha u(x, t) = \frac{1}{\Gamma(1 - \alpha)} \int_0^t (t - \eta)^{-\alpha} \frac{\partial u(x, \eta)}{\partial \eta} d\eta$$

and

$$\frac{\partial^\beta u(x, t)}{\partial |x|^\beta} = -\frac{1}{2 \cos(\beta\pi/2) \Gamma(2 - \beta)} \frac{\partial^2}{\partial x^2} \int_{-\infty}^{\infty} |x - \zeta|^{1-\beta} u(\zeta, t) d\zeta,$$

respectively. Here,  $\Gamma(\cdot)$  is the Gamma function.

Eq. (1.1) can be used to analyze the diffusion images of human brain tissues [14, 15]. It also provides new insights into further investigations of tissue structures and microenvironment. Generally, it is difficult to obtain analytical solutions of fractional partial differential equations (FPDEs). Thus, numerous numerical methods have been proposed to solve them, see [16–25] and references therein. Yang et al. [26] proposed two novel numerical schemes to solve a time-space fractional diffusion equation. Sun et al. [27] constructed two finite difference schemes to solve Eq. (1.1). The unique solvability, unconditional stability and convergence of their schemes are proved. Later, Zhu and Sun [12] considered a high-order scheme for Eq. (1.1). They proved that the convergence orders of their scheme are 3 in time and 4 in space, respectively. Arshad et al. [28] proposed a second-order trapezoidal scheme to solve the time–space fractional diffusion equation. In [29], the authors proposed a numerical scheme by using a finite difference method in time and a finite element method in space to solve the two-dimensional version of Eq. (1.1). Dehghan and Abbaszadeh [30] extended the method in [29] to solve space/multi-time fractional Bloch-Torrey equations. Numerical methods for solving other FPDEs can be found in [31–36].

To our knowledge, we can obtain numerical solutions of FPDEs globally in time by solving the all-at-once systems arising from FPDEs. This advantage attracts many researchers' attentions [19, 37–43]. Lu

et al. [37] proposed an approximate inversion (AI) method to solve the block lower triangular Toeplitz system with tri-diagonal blocks (BL3TB) from fractional sub-diffusion equations. Ke et al. [38] found that if the coefficient matrix in [37] is not exact BL3TB, the AI method will be no longer available. Thus, they [38] proposed another direct method called block divide-and-conquer (BDAC) method for solving the block lower triangular Toeplitz-like system with tri-diagonal block arising from fractional time-dependent partial differential equations. Lin and Ng [41] developed a fast solver based on the BDAC method for the all-at-once system arising from the multidimensional time–space fractional diffusion equation with variable coefficients. Gu and Wu [19] constructed an iterative algorithm for solving Volterra partial integro-differential problems with weakly singular kernel in a parallel-in-time (PinT) pattern. Different from the above mentioned works, Lin et al. [44] developed a two-sided PinT preconditioning method for the all-at-once system from a non-local evolutionary equation with weakly singular kernel. Inspired by this work, in this paper, we design a bilateral preconditioning technique for accelerating a Krylov subspace solver to an L2-type all-at-once system arising from Eq. (1.1).

The rest of this paper is organized as follows. In Section 2, we derive our L2-type all-at-once system for solving Eq. (1.1). In Section 3, we propose our bilateral preconditioning technique and analyze the condition number of the preconditioned matrix. Numerical results are reported in Section 4. Concluding remarks are given in Section 5.

## 2. The L2-type difference scheme and the all-at-once system

In this section, following the idea of [45], we propose an L2-type difference scheme for solving Eq. (1.1). The stability and convergence of our scheme are proved. Based on this scheme, our L2-type all-at-once system is derived.

### 2.1. The L2-type difference scheme and its stability

For two given positive integers  $N$  and  $M$ , let  $h = \frac{x_R - x_L}{N}$  and  $\tau_t = \frac{T}{M}$ . Then, the space  $[x_L, x_R]$  and the time  $[0, T]$  can be discretized uniformly by  $\Omega_h = \{x_i = x_L + ih, 0 \leq i \leq N, x_0 = x_L, x_N = x_R\}$  and  $\Omega_\tau = \{t_j = j\tau_t, 0 \leq j \leq M, t_0 = 0, t_M = T\}$ , respectively.

For approximating the Caputo fractional derivative  ${}_0^C \mathcal{D}_t^\alpha u(x, t)$  in Eq. (1.1), we choose the following L2 formula proposed by Alikhanov and Huang [45].

**Lemma 2.1.** ([45]) *For any  $\alpha \in (0, 1)$  and  $y(t) \in \mathcal{C}^3[0, t_{j+1}]$  ( $j = 1, 2, \dots, M - 1$ ). Then,*

$$\left| {}_0^C \mathcal{D}_{t_{j+1}}^\alpha y(t) - \delta_t^\alpha y(t_{j+1}) \right| = \mathcal{O}(\tau_t^{3-\alpha}),$$

where

$$\delta_t^\alpha y(t_{j+1}) = \frac{\tau_t^{-\alpha}}{\Gamma(2-\alpha)} \sum_{s=0}^j c_{j-s}^{(\alpha)} [y(t_{s+1}) - y(t_s)],$$

and for  $j = 1$ ,

$$c_s^{(\alpha)} = \begin{cases} a_0^{(\alpha)} + b_0^{(\alpha)} + b_1^{(\alpha)}, & s = 0, \\ a_1^{(\alpha)} - b_1^{(\alpha)} - b_0^{(\alpha)}, & s = 1, \end{cases}$$

for  $j = 2$ ,

$$c_s^{(\alpha)} = \begin{cases} a_0^{(\alpha)} + b_0^{(\alpha)}, & s = 0, \\ a_1^{(\alpha)} + b_1^{(\alpha)} + b_2^{(\alpha)} - b_0^{(\alpha)}, & s = 1, \\ a_2^{(\alpha)} - b_2^{(\alpha)} - b_1^{(\alpha)}, & s = 2, \end{cases}$$

for  $j \geq 3$ ,

$$c_s^{(\alpha)} = \begin{cases} a_0^{(\alpha)} + b_0^{(\alpha)}, & s = 0, \\ a_s^{(\alpha)} + b_s^{(\alpha)} - b_{s-1}^{(\alpha)}, & 1 \leq s \leq j-2, \\ a_{j-1}^{(\alpha)} + b_{j-1}^{(\alpha)} + b_j^{(\alpha)} - b_{j-2}^{(\alpha)}, & s = j-1, \\ a_j^{(\alpha)} - b_j^{(\alpha)} - b_{j-1}^{(\alpha)}, & s = j, \end{cases}$$

$$a_\ell^{(\alpha)} = (\ell+1)^{1-\alpha} - \ell^{1-\alpha} \quad (\ell \geq 0) \quad \text{and} \quad b_\ell^{(\alpha)} = \frac{1}{2-\alpha} [(\ell+1)^{2-\alpha} - \ell^{2-\alpha}] - \frac{1}{2} [(\ell+1)^{1-\alpha} + \ell^{1-\alpha}] \quad (\ell \geq 0).$$

Denote

$$\Psi^{2+\alpha}(\mathbb{R}) = \left\{ y \mid \int_{-\infty}^{+\infty} (1+|\omega|)^{2+\alpha} |\hat{y}(\omega)| d\omega < \infty, y \in L^1(\mathbb{R}) \right\},$$

where  $\hat{y}(\omega) = \int_{-\infty}^{+\infty} e^{i\omega t} y(t) dt$  is the Fourier transformation of  $y(t)$  and  $\mathbf{i} = \sqrt{-1}$ . On the other hand, the Riesz fractional derivative  $\frac{\partial^\beta u(x,t)}{\partial |x|^\beta}$  at  $x_i$  can be approximated by the second-order fractional centered difference method [46, 47]. That is, for  $u(x, \cdot) \in \Psi^{2+\alpha}(\mathbb{R})$ , we have

$$\frac{\partial^\beta u(x_i, t)}{\partial |x|^\beta} = -h^{-\beta} \sum_{k=-N+i}^i g_k^\beta u(x_{i-k}, t) + \mathcal{O}(h^2) = \delta_x^\beta u(x_i, t) + \mathcal{O}(h^2), \quad (2.1)$$

where

$$g_k^\beta = \frac{(-1)^k \Gamma(1+\beta)}{\Gamma(\beta/2 - k + 1) \Gamma(\beta/2 + k + 1)}, \quad k \in \mathbb{Z}.$$

Let  $u_i^j$  be the approximation of  $u(x_i, t_j)$  and  $f_i^j = f(x_i, t_j)$ . Combining Lemma 2.1 and Eq. (2.1), the L2-type finite difference scheme of Eq. (1.1) is:

$$\delta_t^\alpha u_i^{j+1} = \kappa \delta_x^\beta u_i^{j+1} + f_i^{j+1} \quad \text{for} \quad 1 \leq i \leq N-1, \quad 1 \leq j \leq M-1 \quad (2.2)$$

with the discretized boundary conditions  $u_0^j = u_N^j = 0$  ( $0 \leq j \leq M$ ) and the initial value  $u_i^0 = \phi(x_i)$  ( $1 \leq i \leq N-1$ ). Notice that the scheme (2.2) is not a self-starting scheme since  $u_i^1$  is unknown. Thus, we need to obtain  $u_i^1$  first by other methods. In this work, we use the following fast L1 scheme [48, 49] to get  $u_i^1$ :

$$\hat{\delta}_t^\alpha \tilde{u}_i^j = \kappa \delta_x^\beta \tilde{u}_i^j + f_i^j \quad \text{for } 1 \leq i \leq N-1, 1 \leq j \leq \hat{M} = \lfloor t_1/\hat{\tau} \rfloor \quad (2.3)$$

with  $\tilde{u}_0^j = u_0^j$ ,  $\tilde{u}_N^j = u_N^j$  and  $\tilde{u}_i^0 = u_i^0$ , where  $\hat{\tau} = \tau_t^{\frac{3-\alpha}{2-\alpha}}$ ,  $u_i^1 = \tilde{u}_i^{\hat{M}}$  and

$$\hat{\delta}_t^\alpha \tilde{u}_i^j = \frac{1}{\Gamma(1-\alpha)} \left[ b_j^{(j,\alpha)} \tilde{u}_i^j - \sum_{k=1}^{j-1} \left( b_{k+1}^{(j,\alpha)} - b_k^{(j,\alpha)} \right) \tilde{u}_i^k - b_1^{(j,\alpha)} \tilde{u}_i^0 \right].$$

Here

$$b_k^{(j,\alpha)} = \begin{cases} \sum_{\ell=1}^{\hat{M}_{exp}} w_\ell \int_{k-1}^k e^{-\hat{\tau} s_\ell (j-s)} ds, & k = 1, 2, \dots, j-1, \\ \frac{\hat{\tau}^{-\alpha}}{1-\alpha}, & k = j, \end{cases}$$

$\hat{M}_{exp} \in \mathbb{N}^+$  and  $w_\ell, s_\ell \geq 0$  ( $\ell = 1, 2, \dots, \hat{M}_{exp}$ ).

For any  $\mathbf{v}, \mathbf{w} \in \mathcal{S} = \{\mathbf{v} | \mathbf{v} = (v_0, v_1, \dots, v_N), v_0 = v_N = 0\}$ , we define an inner product and the corresponding norm:

$$(\mathbf{v}, \mathbf{w}) = h \sum_{i=1}^{N-1} v_i w_i, \quad \|\mathbf{v}\| = \sqrt{(\mathbf{v}, \mathbf{v})}.$$

Let  $\mathbf{u}^j = [u_1^j, u_2^j, \dots, u_{N-1}^j]^T$  and  $\mathbf{f}^j = [f_1^j, f_2^j, \dots, f_{N-1}^j]^T$ . With these at hand, we have the following priori estimate.

**Theorem 2.1.** *Suppose  $u_i^j$  ( $0 \leq i \leq N, 1 \leq j \leq M$ ) be a solution of the scheme (2.2). Then, we have*

$$\tau_t \sum_{j=1}^{M-1} (\|\mathbf{u}^{j+1}\|^2 + \|\Xi^\beta \mathbf{u}^{j+1}\|^2) \leq C_1 \left( \|\mathbf{u}^1\|^2 + \|\mathbf{u}^0\|^2 + \tau_t \sum_{j=1}^{M-1} \|\mathbf{f}^{j+1}\|^2 \right),$$

where  $\Xi^\beta$  is the square root of  $-\delta_x^\beta$ , and  $C_1$  is a positive constant independent of  $\tau_t$  and  $h$ .

*Proof.* This proof is similar to the proof of Theorem 3.1 in [45]. Thus, we omit it here. It is worth mentioning that in this proof, the property given as follows is used:

$$(-\delta_x^\beta \mathbf{u}^j, \mathbf{u}^j) = \|\Xi^\beta \mathbf{u}^j\|^2 \geq c_*^\beta (x_R - x_L)^{-\beta} \|\mathbf{u}^j\|^2,$$

where  $c_*^\beta = 2e^{-2} \frac{(4-\beta)(2-\beta)\Gamma(\beta+1)}{(6+\beta)(4+\beta)(2+\beta)\Gamma^2(\beta/2+1)} (3/2 + \beta/4)^{\beta+1}$ , see [27, 50] for details.  $\square$

Based on Theorem 2.1, the stability and the convergence of (2.2) can be proved without difficulty.

## 2.2. The L2-type all-at-once system

In this subsection, we derive our L2-type all-at-once system based on the scheme (2.2). Firstly, we rewrite it into the matrix form:

$$\frac{h^\beta \tau_t^{-\alpha}}{\Gamma(2-\alpha)} \sum_{s=0}^j c_{j-s}^{(\alpha)} (\mathbf{u}^{s+1} - \mathbf{u}^s) + \kappa G_\beta \mathbf{u}^{j+1} = h^\beta \mathbf{f}^{j+1}, \quad (2.4)$$

where

$$G_\beta = \begin{bmatrix} g_0^\beta & g_{-1}^\beta & g_{-2}^\beta & \cdots & g_{3-N}^\beta & g_{2-N}^\beta \\ g_1^\beta & g_0^\beta & g_{-1}^\beta & g_{-2}^\beta & \cdots & g_{3-N}^\beta \\ \vdots & g_1^\beta & g_0^\beta & \ddots & \ddots & \vdots \\ \vdots & \ddots & \ddots & \ddots & \ddots & g_{-2}^\beta \\ g_{N-3}^\beta & \ddots & \ddots & \ddots & g_0^\beta & g_{-1}^\beta \\ g_{N-2}^\beta & g_{N-3}^\beta & \cdots & \cdots & g_1^\beta & g_0^\beta \end{bmatrix}$$

is a symmetric positive definite Toeplitz matrix [47].

Before deriving our all-at-once system, some notations are introduced:  $\mathbf{0}$  is a zero matrix with suitable size,  $I_t$  and  $I_x$  are two identity matrices with orders  $M-1$  and  $N-1$ , respectively. Denote

$$\mathbf{u} = [(\mathbf{u}^2)^T, (\mathbf{u}^3)^T, \dots, (\mathbf{u}^M)^T]^T \quad \text{and} \quad \mathbf{f} = [(\mathbf{f}^2)^T, (\mathbf{f}^3)^T, \dots, (\mathbf{f}^M)^T]^T.$$

To avoid the misunderstanding, we also denote  $\tilde{c}_0^{(\alpha)} = a_0^{(\alpha)} + b_0^{(\alpha)} + b_1^{(\alpha)}$ ,

$$\tilde{c}_k^{(\alpha)} = a_k^{(\alpha)} + b_k^{(\alpha)} + b_{k+1}^{(\alpha)} - b_{k-1}^{(\alpha)}, \quad \hat{c}_k^{(\alpha)} = a_k^{(\alpha)} - b_k^{(\alpha)} - b_{k-1}^{(\alpha)}, \quad k = 1, 2, \dots, M-1.$$

Then, let  $A_{11} = \frac{h^\beta \tau_t^{-\alpha}}{\Gamma(2-\alpha)} \tilde{c}_0^{(\alpha)}$ ,  $A_{12} = \frac{h^\beta \tau_t^{-\alpha}}{\Gamma(2-\alpha)} [\tilde{c}_1^{(\alpha)} - c_0^{(\alpha)}, \tilde{c}_2^{(\alpha)} - c_1^{(\alpha)}, \dots, \tilde{c}_{M-2}^{(\alpha)} - c_{M-3}^{(\alpha)}]^T$  and

$$A_{22} = \frac{h^\beta \tau_t^{-\alpha}}{\Gamma(2-\alpha)} \begin{bmatrix} c_0^{(\alpha)} & 0 & \cdots & \cdots & 0 \\ c_1^{(\alpha)} - c_0^{(\alpha)} & c_0^{(\alpha)} & \ddots & \ddots & \vdots \\ \ddots & \ddots & \ddots & \ddots & 0 \\ \ddots & \ddots & \ddots & c_0^{(\alpha)} & 0 \\ c_{M-3}^{(\alpha)} - c_{M-4}^{(\alpha)} & \cdots & \cdots & c_1^{(\alpha)} - c_0^{(\alpha)} & c_0^{(\alpha)} \end{bmatrix}.$$

Here  $c_0^{(\alpha)} = a_0^{(\alpha)} + b_0^{(\alpha)}$  and  $c_s^{(\alpha)} = a_s^{(\alpha)} + b_s^{(\alpha)} - b_{s-1}^{(\alpha)}$  ( $s = 1, \dots, M-3$ ).

With the help of Eq. (2.4) and the above notations, the all-at-once system is written as:

$$\mathcal{M} \mathbf{u} = -\boldsymbol{\eta} + h^\beta \mathbf{f}, \quad (2.5)$$

where  $\mathcal{M} = A_t \otimes I_x + I_t \otimes (\kappa G_\beta)$  with

$$A_t = \begin{bmatrix} A_{11} & \mathbf{0} \\ A_{12} & A_{22} \end{bmatrix}$$

and

$$\boldsymbol{\eta} = \frac{h^\beta \tau_t^{-\alpha}}{\Gamma(2-\alpha)} \begin{bmatrix} \hat{c}_1^{(\alpha)} (\mathbf{u}^1 - \mathbf{u}^0) - \tilde{c}_0^{(\alpha)} \mathbf{u}^1 \\ \hat{c}_2^{(\alpha)} (\mathbf{u}^1 - \mathbf{u}^0) - \tilde{c}_1^{(\alpha)} \mathbf{u}^1 \\ \vdots \\ \hat{c}_{M-1}^{(\alpha)} (\mathbf{u}^1 - \mathbf{u}^0) - \tilde{c}_{M-2}^{(\alpha)} \mathbf{u}^1 \end{bmatrix}.$$

Some fast algorithms are designed based on the system (2.5), see [19, 43]. However, inspired by [44], in this work, we concentrate on another version of (2.5). More precisely, after doing a permutation transformation of  $\mathbf{u}$ ,  $\boldsymbol{\eta}$  and  $\mathbf{f}$ , we have

$$\tilde{\mathcal{M}}\tilde{\mathbf{u}} = -\tilde{\boldsymbol{\eta}} + h^\beta \tilde{\mathbf{f}}, \quad (2.6)$$

where  $\tilde{\mathcal{M}} = (\kappa G_\beta) \otimes I_t + I_x \otimes A_t$ . Notice that the order of the Kronecker product in  $\mathcal{M}$  is changed. In the next section, a bilateral preconditioning technique is proposed to fast solve Eq. (2.6).

### 3. A bilateral preconditioning and the condition number of the preconditioned matrix

If we use the Gaussian elimination based block forward substitution method [39] to solve Eq. (2.6), the storage requirement and the computational complexity of this method are  $\mathcal{O}(NM^3 + NM^2)$  and  $\mathcal{O}(M^2)$ , respectively. To reduce the computational cost and accelerate solving Eq. (2.6), a bilateral preconditioning strategy is proposed in this section.

#### 3.1. The bilateral preconditioning technique and its implementation

Following the idea of [44], our left and right preconditioners can be written as follows:

$$P_l = (\kappa G_\tau)^{-\frac{1}{2}} \otimes A_t + (\kappa G_\tau)^{\frac{1}{2}} \otimes I_t \quad (3.1)$$

and

$$P_r = (\kappa G_\tau)^{\frac{1}{2}} \otimes I_t, \quad (3.2)$$

respectively. Here,  $G_\tau = G_\beta - H_\beta$  is a  $\tau$ -matrix [51], where  $H_\beta$  is a Hankel matrix and its antidiagonals are given by

$$\left[ g_2^\beta, g_3^\beta, \dots, g_{N-2}^\beta, 0, 0, 0, g_{N-2}^\beta, \dots, g_3^\beta, g_2^\beta \right]^T.$$

Then, the bilateral preconditioned form of Eq. (2.6) is

$$\begin{cases} P_l^{-1} \tilde{\mathcal{M}} P_r^{-1} \hat{\mathbf{u}} = P_l^{-1} \left( -\tilde{\boldsymbol{\eta}} + h^\beta \hat{\mathbf{f}} \right), \\ \tilde{\mathbf{u}} = P_r^{-1} \hat{\mathbf{u}}. \end{cases} \quad (3.3)$$

We know that an  $N \times N$  Toeplitz matrix multiplies a vector can be done by fast Fourier transform (FFT) with  $\mathcal{O}(N \log N)$  operations [52]. Thanks to the Toeplitz structure of  $A_{22}$  and  $G_\beta$ , we choose a Krylov subspace method [53] (e.g., the BiCGSTAB method [54]) to solve Eq. (3.3). In a Krylov subspace method, we have to compute the underlying matrix-vector product. Thus, in the next, we aim to show how to compute the matrix-vector product  $P_l^{-1} \tilde{\mathcal{M}} P_r^{-1} \mathbf{v}$  ( $\mathbf{v}$  is a vector with suitable size) efficiently.

Obviously, the product  $\mathbf{z} = P_l^{-1} \tilde{\mathcal{M}} P_r^{-1} \mathbf{v}$  can be split into the following three sub-steps:

$$\begin{cases} \mathbf{v}_1 = P_r^{-1} \mathbf{v}, & \text{Step1,} \\ \mathbf{v}_2 = \tilde{\mathcal{M}} \mathbf{v}_1, & \text{Step2,} \\ \mathbf{z} = P_l^{-1} \mathbf{v}_2, & \text{Step3.} \end{cases} \quad (3.4)$$

From [51], we know that the  $\tau$ -matrix  $G_\tau$  can be diagonalized as follows:

$$G_\tau = Q_x^T D_\tau Q_x,$$

where  $D_\tau = \text{diag}(\lambda_{\tau,1}, \lambda_{\tau,2}, \dots, \lambda_{\tau,N-1})$  is a diagonal matrix containing all eigenvalues of  $G_\tau$ , and

$$Q_x = \left( \sqrt{2/N} \sin \left( \frac{ij\pi}{N} \right) \right)_{1 \leq i,j \leq N-1}$$

is the sine transform matrix. With this decomposition, Step1 in Eq. (3.4) can be fast implemented in the following way:

$$\mathbf{v}_1 = P_r^{-1} \mathbf{v} = (Q_x^T \otimes I_t) \left[ (\kappa D_\tau)^{-\frac{1}{2}} \otimes I_t \right] (Q_x \otimes I_t) \mathbf{v}.$$

Benefiting from properties of Kronecker product and Lemma 6 in [44], the storage requirement and the computational cost in Step1 are  $\mathcal{O}(MN)$  and  $\mathcal{O}(MN \log N)$ , respectively. As for Step2 in Eq. (3.4),  $\tilde{\mathcal{M}} \mathbf{z}_1$  can be computed by using FFT since  $A_{22}$  and  $G_\beta$  are two Toeplitz matrices. Thus, the computational complexity and the storage requirement in Step2 are  $\mathcal{O}(MN \log(MN))$  and  $\mathcal{O}(MN)$ , respectively.

Compared with the previous two steps (i.e., Step1 and Step2), the third step is a little more complicated. Using the diagonalization of  $G_\tau$ , we can rewrite  $P_l$  as:

$$P_l = (Q_x^T \otimes I_t) \left[ (\kappa D_\tau)^{\frac{1}{2}} \otimes I_t + (\kappa D_\tau)^{-\frac{1}{2}} \otimes A_t \right] (Q_x \otimes I_t).$$

Denote

$$\Sigma_i = (\kappa \lambda_{\tau,i})^{\frac{1}{2}} I_t + (\kappa \lambda_{\tau,i})^{-\frac{1}{2}} A_t, \quad \text{for } i = 1, 2, \dots, N-1.$$

The product  $\mathbf{z} = P_l^{-1} \mathbf{v}_2$  can be calculated via the following three steps:

$$\begin{cases} \mathbf{z}_1 = (Q_x \otimes I_t) \mathbf{v}, & \text{Step-(a),} \\ \Sigma_n \mathbf{z}_{2,n} = \mathbf{z}_{1,n}, \quad 1 \leq n \leq N-1, & \text{Step-(b),} \\ \mathbf{z} = (Q_x^T \otimes I_t) \mathbf{z}_2, & \text{Step-(c),} \end{cases} \quad (3.5)$$

where  $\mathbf{z}_j = [\mathbf{z}_{j,1}^T, \mathbf{z}_{j,2}^T, \dots, \mathbf{z}_{j,N-1}^T]^T$  with  $j = 1, 2$ . Note that  $\Sigma_i$  ( $1 \leq i \leq N-1$ ) are 2-by-2 block matrices, i.e.,

$$\Sigma_i = \begin{bmatrix} \Sigma_{i,11} & \mathbf{0} \\ \Sigma_{i,12} & \Sigma_{i,22} \end{bmatrix},$$

where

$$\Sigma_{i,11} = (\kappa \lambda_{\tau,i})^{\frac{1}{2}} I_{t1} + (\kappa \lambda_{\tau,i})^{-\frac{1}{2}} A_{11}, \quad \Sigma_{i,12} = (\kappa \lambda_{\tau,i})^{-\frac{1}{2}} A_{12}, \quad \Sigma_{i,22} = (\kappa \lambda_{\tau,i})^{\frac{1}{2}} I_{t2} + (\kappa \lambda_{\tau,i})^{-\frac{1}{2}} A_{22}$$

and  $\text{blkdiag}(I_{t1}, I_{t2}) = I_t$ . Then, we have  $\mathbf{z}_{2,n} = \Sigma_n^{-1} \mathbf{z}_{1,n}$  for  $1 \leq n \leq N-1$ , where

$$\Sigma_n^{-1} = \begin{bmatrix} \Sigma_{n,11}^{-1} & \mathbf{0} \\ -\Sigma_{n,22}^{-1} \Sigma_{n,12} \Sigma_{n,11}^{-1} & \Sigma_{n,22}^{-1} \end{bmatrix}.$$

From [55], we know that the inverse of an invertible lower triangular Toeplitz matrix is also an invertible lower triangular Toeplitz matrix. Thus, we choose the modified version of Bini's algorithm [56] to compute  $\Sigma_{n,22}^{-1}$ . The computational cost and the storage requirement of (3.5) are  $\mathcal{O}(MN \log(MN))$  and  $\mathcal{O}(MN)$ , respectively. Consequently, the computation of (3.3) requires  $\mathcal{O}(MN \log(MN))$  flops. It is worth remarking that the invertibilities of  $P_l$  and  $P_r$  are not discussed. We leave it to the following subsection.

### 3.2. The condition number of the preconditioned matrix

In this subsection, we show the nonsingularities of  $P_l$  and  $P_r$ , and estimate the condition number of the preconditioned matrix  $P_l^{-1} \tilde{\mathcal{M}} P_r^{-1}$ .

Firstly, we prove that  $A_t + A_t^T$  is positive definite. Before doing this, the following properties are needed.

**Lemma 3.1.** ([57]) *For  $\alpha \in (0, 1)$ , it holds*

- (i)  $a_k^{(\alpha)} > 0$  ( $k \geq 0$ ) and  $a_0^{(\alpha)} > a_1^{(\alpha)} > \dots$ ;
- (ii)  $b_k^{(\alpha)} > 0$  ( $k \geq 0$ ) and  $b_0^{(\alpha)} > b_1^{(\alpha)} > \dots$

**Lemma 3.2.** For  $\alpha \in (0, 0.3624)$ , we have

(i)  $c_k^{(\alpha)} > 0$  and  $c_{k+1}^{(\alpha)} - c_k^{(\alpha)} < 0$  for  $k = 0, 1, \dots$ ;

(ii)  $\tilde{c}_k^{(\alpha)} > 0$  and  $\tilde{c}_{k+1}^{(\alpha)} - c_k^{(\alpha)} < 0$  for  $k = 0, 1, \dots$

*Proof.* According to the proof of Lemma 2.2 in [57], we obtain that for  $\alpha \in (0, 0.3624)$ ,  $c_k^{(\alpha)} > 0$  ( $k = 0, 1, \dots$ ),  $c_1^{(\alpha)} - c_0^{(\alpha)} < 0$  and  $c_{k+1}^{(\alpha)} - c_k^{(\alpha)} < 0$  ( $k = 2, 3, \dots$ ). From Fig. 1(a), we have  $c_2^{(\alpha)} - c_1^{(\alpha)} < 0$  for  $\alpha \in (0, 0.3624)$ . Thus, the first property is true.

It is easy to check that  $\tilde{c}_k^{(\alpha)} > 0$  ( $k = 0, 1, \dots$ ) since  $\tilde{c}_k^{(\alpha)} = c_k^{(\alpha)} + b_{k+1}^{(\alpha)}$ . Now, we remain to show  $\tilde{c}_{k+1}^{(\alpha)} - c_k^{(\alpha)} < 0$ . Using Lemma 3.1, we have

$$\tilde{c}_1^{(\alpha)} - c_0^{(\alpha)} = a_1^{(\alpha)} - a_0^{(\alpha)} + b_1^{(\alpha)} - b_0^{(\alpha)} + b_2^{(\alpha)} - b_0^{(\alpha)} < 0.$$

Based on the proof of Lemma 2.3 in [45], we get  $\tilde{c}_{k+1}^{(\alpha)} - c_k^{(\alpha)} < 0$  ( $k = 2, 3, \dots$ ). Clearly, we can see from Fig. 1(b) that for  $\alpha \in (0, 0.3624)$ ,  $\tilde{c}_2^{(\alpha)} - c_1^{(\alpha)} < 0$ . The proof is completed.  $\square$

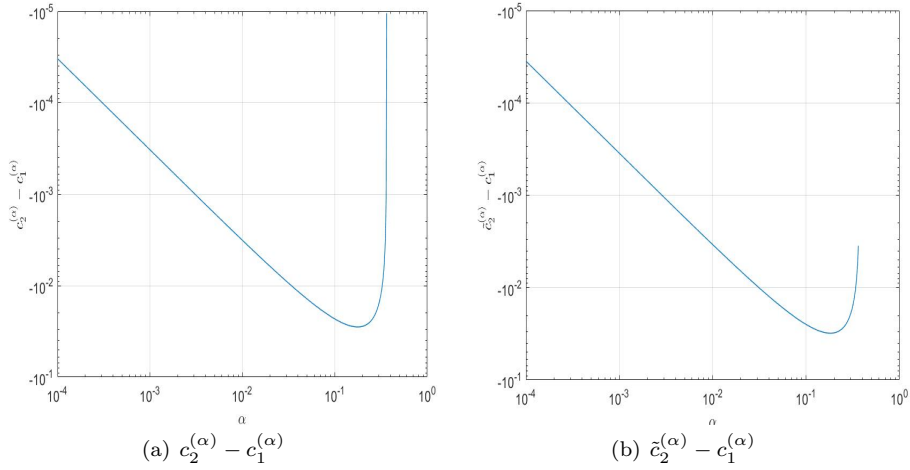


Fig. 1: The values of  $c_2^{(\alpha)} - c_1^{(\alpha)}$  and  $\tilde{c}_2^{(\alpha)} - c_1^{(\alpha)}$  for  $\alpha \in (0, 0.3624)$ .

With these at hand, we get the following result.

**Theorem 3.1.** For any  $\alpha \in (0, 0.3624)$ , the matrix  $A_t + A_t^T$  is positive definite.

*Proof.* According to Lemma 3.2 and Gershgorin circle theorem [58], the first Gershgorin disc of the matrix

$A_t + A_t^T$  is centered at  $\frac{2h^\beta \tau_t^{-\alpha}}{\Gamma(2-\alpha)} \tilde{c}_0^{(\alpha)} > 0$  with radius

$$\begin{aligned} R_1 &= \frac{h^\beta \tau_t^{-\alpha}}{\Gamma(2-\alpha)} \sum_{k=1}^{M-2} \left| \tilde{c}_k^{(\alpha)} - c_{k-1}^{(\alpha)} \right| = \frac{h^\beta \tau_t^{-\alpha}}{\Gamma(2-\alpha)} \left( c_0^{(\alpha)} + \sum_{k=1}^{M-3} c_k^{(\alpha)} - \sum_{k=1}^{M-2} \tilde{c}_k^{(\alpha)} \right) \\ &< \frac{h^\beta \tau_t^{-\alpha}}{\Gamma(2-\alpha)} \left[ c_0^{(\alpha)} + \sum_{k=1}^{M-2} \left( c_k^{(\alpha)} - \tilde{c}_k^{(\alpha)} \right) \right] = \frac{h^\beta \tau_t^{-\alpha}}{\Gamma(2-\alpha)} \left( c_0^{(\alpha)} - \sum_{k=2}^{M-1} b_k^{(\alpha)} \right) < \frac{2h^\beta \tau_t^{-\alpha}}{\Gamma(2-\alpha)} \tilde{c}_0^{(\alpha)}. \end{aligned}$$

The  $j$ th ( $2 \leq j \leq M-1$ ) Gershgorin disc is centered at  $\frac{2h^\beta \tau_t^{-\alpha}}{\Gamma(2-\alpha)} c_0^{(\alpha)} > 0$  with radius

$$\begin{aligned} R_j &= \frac{h^\beta \tau_t^{-\alpha}}{\Gamma(2-\alpha)} \left( \left| \tilde{c}_{j-1}^{(\alpha)} - c_{j-2}^{(\alpha)} \right| + \sum_{k=1}^{j-2} \left| c_k^{(\alpha)} - c_{k-1}^{(\alpha)} \right| + \sum_{k=1}^{M-j-1} \left| c_k^{(\alpha)} - c_{k-1}^{(\alpha)} \right| \right) \\ &= \frac{h^\beta \tau_t^{-\alpha}}{\Gamma(2-\alpha)} \left[ c_{j-2}^{(\alpha)} - \tilde{c}_{j-1}^{(\alpha)} + \sum_{k=1}^{j-2} \left( c_{k-1}^{(\alpha)} - c_k^{(\alpha)} \right) + \sum_{k=1}^{M-j-1} \left( c_{k-1}^{(\alpha)} - c_k^{(\alpha)} \right) \right] \\ &= \frac{h^\beta \tau_t^{-\alpha}}{\Gamma(2-\alpha)} \left( 2c_0^{(\alpha)} - \tilde{c}_{j-1}^{(\alpha)} - c_{M-j-1}^{(\alpha)} \right) < \frac{2h^\beta \tau_t^{-\alpha}}{\Gamma(2-\alpha)} c_0^{(\alpha)}. \end{aligned}$$

This implies that all eigenvalues of  $A_t + A_t^T$  are positive. Thus, the matrix  $A_t + A_t^T$  is positive definite.  $\square$

We review some properties of  $g_k^\beta$ . It will be used later.

**Lemma 3.3.** ([47]) *Suppose  $\beta \in (1, 2)$ , we have*

$$(i) \quad g_0^\beta \geq 0 \text{ and } g_k^\beta = g_{-k}^\beta \text{ for } |k| \geq 1;$$

$$(ii) \quad g_0^\beta + 2 \sum_{k=1}^{N-2} g_k^\beta > 0.$$

**Theorem 3.2.** *For any  $\alpha \in (0, 1)$  and  $\beta \in (1, 2)$ , the matrices  $P_l$  and  $P_r$  are nonsingular.*

*Proof.* Combining Lemma 3.2 in [59] and Lemma 3.3, we have  $\lambda_{\tau,i} > 0$  for  $1 \leq i \leq N-1$ . Then,  $P_r$  is nonsingular. Noticing that  $(\kappa D_\tau)^{\frac{1}{2}} \otimes I_t + (\kappa D_\tau)^{-\frac{1}{2}} \otimes A_t$  is a lower triangular matrix with its all diagonal entries are positive. Thus,  $P_l$  is nonsingular and the proof is completed.  $\square$

The proof of Theorem 3.2 implies that the matrix  $G_\tau$  is symmetric positive definite. We turn to show the boundedness of the spectrum of  $G_\tau^{-1} G_\beta$ . Let  $h_{ij}$  and  $\tilde{g}_{ij}$  be the entries of  $H_\beta$  and  $G_\tau$ , respectively. Then, we get

$$h_{ij} = \begin{cases} g_{i+j}^\beta, & i+j < N-2, \\ 0, & i+j = N-2, N-1, N, \\ g_{2N-(i+j)}^\beta, & \text{others,} \end{cases}$$

and  $\tilde{g}_{ij} = g_{|i-j|}^\beta - h_{ij}$ . Similar to [59, Lemma 4.2], we know that

$$p_{ii} > 0 \text{ and } p_{ij} < 0 \quad \text{for } 1 \leq i, j \leq N-1, i \neq j. \quad (3.6)$$

**Theorem 3.3.** *The spectrum of  $G_\tau^{-1}G_\beta$  is uniformly bounded, and we have*

$$\frac{1}{2} < \lambda(G_\tau^{-1}G_\beta) < \frac{3}{2},$$

where  $\lambda(G_\tau^{-1}G_\beta)$  represents the eigenvalues of  $G_\tau^{-1}G_\beta$ .

*Proof.* This proof is slightly different to [59, Theorem 4.4]. Thus, we omit it here.  $\square$

For any real symmetric matrices  $D_1, D_2 \in \mathbb{R}^{n \times n}$ , we denote  $D_1 \succ$  (or  $\succeq$ )  $D_2$  if  $D_1 - D_2$  is positive definite (or semi-definite). Then, we have the following properties.

**Lemma 3.4.** (i)  $\mathbf{0} \prec \frac{1}{2}G_\tau \prec G_\beta \prec \frac{3}{2}G_\tau$ ;

(ii)  $\frac{1}{2}I_x \prec G_\tau^{-\frac{1}{2}}G_\beta G_\tau^{-\frac{1}{2}} \prec \frac{3}{2}I_x$ .

*Proof.* By the Rayleigh quotients theorem [60, Theorem 4.2.2] and Theorem 3.3, we have

$$\frac{1}{2} < \frac{\mathbf{z}^T G_\beta \mathbf{z}}{\mathbf{z}^T G_\tau \mathbf{z}} < \frac{3}{2},$$

where  $\mathbf{z} \in \mathbb{R}^{N-1}$  is an arbitrary nonzero vector. That is,

$$\frac{1}{2} \mathbf{z}^T G_\tau \mathbf{z} < \mathbf{z}^T G_\beta \mathbf{z} < \frac{3}{2} \mathbf{z}^T G_\tau \mathbf{z}.$$

Then, we get

$$\mathbf{0} \prec \frac{1}{2}G_\tau \prec G_\beta \prec \frac{3}{2}G_\tau.$$

On the other hand,

$$\frac{1}{2} < \frac{\mathbf{z}^T G_\tau^{-\frac{1}{2}} G_\beta G_\tau^{-\frac{1}{2}} \mathbf{z}}{\mathbf{z}^T \mathbf{z}} = \frac{\mathbf{y}^T G_\beta \mathbf{y}}{\mathbf{y}^T G_\tau \mathbf{y}} < \frac{3}{2}.$$

This implies (ii) and the proof is completed.  $\square$

For estimating the condition number of  $P_l^{-1} \tilde{\mathcal{M}} P_r^{-1}$ , another two auxiliary lemmas are needed.

**Lemma 3.5.** ([44]) *Let  $B_1, B_2 \in \mathbb{R}^{n \times n}$  be symmetric matrices such that  $\mathbf{0} \prec B_1 \preceq B_2$ . Then,  $\mathbf{0} \prec B_2^{-1} \preceq B_1^{-1}$ .*

**Lemma 3.6.** ([44]) For positive numbers  $\xi_k, \eta_k$  ( $1 \leq k \leq n$ ), it holds that

$$\min_{1 \leq k \leq n} \frac{\xi_k}{\eta_k} \leq \left( \sum_{k=1}^n \eta_k \right)^{-1} \left( \sum_{k=1}^n \xi_k \right) \leq \max_{1 \leq k \leq n} \frac{\xi_k}{\eta_k}.$$

For an arbitrary nonsingular matrix  $A$ , we define its condition number as

$$\kappa_2(A) = \|A^{-1}\|_2 \|A\|_2.$$

Now, we are in position to estimate  $\kappa_2(P_l^{-1} \tilde{\mathcal{M}} P_r^{-1})$ .

**Theorem 3.4.** For any  $\alpha \in (0, 0.3624)$ , the condition number of  $P_l^{-1} \tilde{\mathcal{M}} P_r^{-1}$  is bounded, i.e.,

$$\kappa_2(P_l^{-1} \tilde{\mathcal{M}} P_r^{-1}) < 2\sqrt{3}.$$

*Proof.* Denote  $\hat{\mathcal{M}} = (\kappa G_\beta)^{\frac{1}{2}} \otimes I_t + (\kappa G_\beta)^{-\frac{1}{2}} \otimes A_t$ . Then, we have

$$\tilde{\mathcal{M}} = \hat{\mathcal{M}} \left[ (\kappa G_\beta)^{\frac{1}{2}} \otimes I_t \right]$$

and

$$\left( P_l^{-1} \tilde{\mathcal{M}} P_r^{-1} \right) \left( P_l^{-1} \tilde{\mathcal{M}} P_r^{-1} \right)^T = P_l^{-1} \hat{\mathcal{M}} \left\{ \left[ (\kappa G_\beta)^{\frac{1}{2}} (\kappa G_\tau)^{-1} (\kappa G_\beta)^{\frac{1}{2}} \right] \otimes I_t \right\} \hat{\mathcal{M}}^T P_l^{-T}. \quad (3.7)$$

We notice that the matrix  $\left[ (\kappa G_\beta)^{\frac{1}{2}} (\kappa G_\tau)^{-1} (\kappa G_\beta)^{\frac{1}{2}} \right] \otimes I_t$  is similar to  $\left[ (\kappa G_\tau)^{-\frac{1}{2}} (\kappa G_\beta) (\kappa G_\tau)^{-\frac{1}{2}} \right] \otimes I_t$ . Using Lemma 3.4(ii), we obtain

$$\frac{1}{2} I_{xt} \prec \left[ (\kappa G_\beta)^{\frac{1}{2}} (\kappa G_\tau)^{-1} (\kappa G_\beta)^{\frac{1}{2}} \right] \otimes I_t \prec \frac{3}{2} I_{xt},$$

where  $I_{xt} = I_x \otimes I_t$ . Bring this estimate into Eq. (3.7), we get

$$\frac{1}{2} P_l^{-1} \hat{\mathcal{M}} \hat{\mathcal{M}}^T P_l^{-T} \prec \left( P_l^{-1} \tilde{\mathcal{M}} P_r^{-1} \right) \left( P_l^{-1} \tilde{\mathcal{M}} P_r^{-1} \right)^T \prec \frac{3}{2} P_l^{-1} \hat{\mathcal{M}} \hat{\mathcal{M}}^T P_l^{-T}. \quad (3.8)$$

Now, it remains to give a bound of the matrix  $P_l^{-1} \hat{\mathcal{M}} \hat{\mathcal{M}}^T P_l^{-T}$ . Let  $\mathbf{z} \in \mathbb{R}^{N-1}$  be an arbitrary nonzero vector. Then, the Rayleigh quotient of  $P_l^{-1} \hat{\mathcal{M}} \hat{\mathcal{M}}^T P_l^{-T}$  is

$$\begin{aligned} \frac{\mathbf{z}^T P_l^{-1} \hat{\mathcal{M}} \hat{\mathcal{M}}^T P_l^{-T} \mathbf{z}}{\mathbf{z}^T \mathbf{z}} &= \frac{\mathbf{y}^T P_l^{-T} \mathbf{z}}{\mathbf{y}^T P_l P_l^T \mathbf{y}} \frac{\mathbf{y}^T \hat{\mathcal{M}} \hat{\mathcal{M}}^T \mathbf{y}}{\mathbf{y}^T P_l P_l^T \mathbf{y}} \\ &= \frac{\mathbf{y}^T \left[ (\kappa G_\beta) \otimes I_t + I_x \otimes (A_t + A_t^T) + (\kappa G_\beta)^{-1} \otimes (A_t A_t^T) \right] \mathbf{y}}{\mathbf{y}^T \left[ (\kappa G_\tau) \otimes I_t + I_x \otimes (A_t + A_t^T) + (\kappa G_\tau)^{-1} \otimes (A_t A_t^T) \right] \mathbf{y}}. \end{aligned} \quad (3.9)$$

It is easy to check that  $A_t A_t^T \succ \mathbf{0}$  since  $A_t$  is a lower triangular matrix with its all diagonal entries are

positive. Moreover, from Theorem 3.1 we know that for any  $\alpha \in (0, 0.3624)$ , the matrix  $A_t + A_t^T$  is positive definite. Thus, we can apply Lemma 3.6 to estimate Eq. (3.9).

On the one hand, adopting Lemma 3.4(i), we have

$$\frac{1}{2} < \frac{\mathbf{y}^T [(\kappa G_\beta) \otimes I_t] \mathbf{y}}{\mathbf{y}^T [(\kappa G_\tau) \otimes I_t] \mathbf{y}} < \frac{3}{2}. \quad (3.10)$$

On the other hand, combining Lemma 3.4(i) and Lemma 3.5, we get

$$\frac{2}{3} < \frac{\mathbf{y}^T [(\kappa G_\beta)^{-1} \otimes (A_t A_t^T)] \mathbf{y}}{\mathbf{y}^T [(\kappa G_\tau)^{-1} \otimes (A_t A_t^T)] \mathbf{y}} < 2. \quad (3.11)$$

Applying Lemma 3.6 to Eq. (3.9), we have

$$\frac{1}{2} = \min \left\{ \frac{1}{2}, 1, \frac{2}{3} \right\} < \frac{\mathbf{z}^T P_l^{-1} \hat{\mathcal{M}} \hat{\mathcal{M}}^T P_l^{-T} \mathbf{z}}{\mathbf{z}^T \mathbf{z}} < \max \left\{ \frac{3}{2}, 1, 2 \right\} = 2,$$

where Eqs. (3.10) and (3.11) are used. Then, we have

$$\frac{1}{4} I_{xt} \prec \left( P_l^{-1} \tilde{\mathcal{M}} P_r^{-1} \right) \left( P_l^{-1} \tilde{\mathcal{M}} P_r^{-1} \right)^T \prec 3 I_{xt}.$$

This implies that

$$\kappa_2(P_l^{-1} \tilde{\mathcal{M}} P_r^{-1}) < \sqrt{3 / \left( \frac{1}{4} \right)} = 2\sqrt{3}.$$

□

**Remark 1.** In Eq. (2.6), we can calculate  $\mathbf{u}^2$  first. Then, the rest part has block lower Toeplitz with Toeplitz blocks structure. Following this way, we may loosen the restriction of  $\alpha$  in Theorem 3.4. However, we have to design another preconditioner iterative method for obtaining  $\mathbf{u}^2$ . On the other hand, our idea has another benefit: it can be extended to graded time steps such as [43].

#### 4. Numerical experiments

In this section, we report three examples. Example 1 shows the time and space convergence orders of the scheme (2.2). The performance of our preconditioners in Section 3 is displayed in Example 2. We extend the bilateral preconditioning technique to two space dimensions, and the corresponding results are reported in Example 3. Denote

$$Err_\infty(h, \tau) = \max_{0 \leq i \leq N, 1 \leq j \leq M} |e_i^j|, \quad Err_2(h, \tau) = \max_{1 \leq j \leq M} \|\mathbf{e}^j\|,$$

where  $e_i^j = u(x_i, t_j) - u_i^j$  and  $\mathbf{e}^j = [e_0^j, \dots, e_N^j]^T$ . Then, we denote

$$CO_{\infty, \tau} = \log_{\tau_1/\tau_2} \frac{Err_{\infty}(h, \tau_1)}{Err_{\infty}(h, \tau_2)}, \quad CO_{2, \tau} = \log_{\tau_1/\tau_2} \frac{Err_2(h, \tau_1)}{Err_2(h, \tau_2)},$$

$$CO_{\infty, h} = \log_{h_1/h_2} \frac{Err_{\infty}(h_1, \tau)}{Err_{\infty}(h_2, \tau)}, \quad CO_{2, h} = \log_{h_1/h_2} \frac{Err_2(h_1, \tau)}{Err_2(h_2, \tau)}.$$

Some other notations that will appear later are collected here: “BFSM” and “BS” mean that MATLAB’s backslash operator is used to solve Eqs. (2.2) and (2.6), respectively. “ $\mathcal{T}$ ” and “ $\mathcal{P}$ ” mean that Eq. (2.6) is solved by the BiCGSTAB method and the preconditioned BiCGSTAB (called PBiCGSTAB) method, respectively. “Time” is the total CPU time in seconds for solving the system (2.6). “Iter1” represents the number of iterations required by the (P)CG (PCG means preconditioned CG) method [53] for solving the fast L1 scheme (2.3). “Iter2” is the number of iterations required by the (P)BiCGSTAB method for solving Eq. (2.6). The chosen Krylov subspace method is terminated if the relative residual error satisfies  $\frac{\|\mathbf{r}^{(k)}\|}{\|\mathbf{r}^{(0)}\|} \leq 10^{-9}$  or the iteration number is more than 1000, where  $\mathbf{r}^{(k)}$  denotes the residual vector in the  $k$ th iteration. The initial guess is chosen as the zero vector. Moreover, the generalized minimum residual method [53] is not considered in this work, since it requires large amounts of storage due to the orthogonalization process.

All experiments were performed on a Windows 7 (64 bit) PC-AMD PRO A10-8750B R7 CPU 3.60GHz, 16 GB of RAM using MATLAB R2017b.

**Remark 2.** *It is easy to check that the coefficient matrix of (2.3) is a time-independent symmetric positive definite Toeplitz matrix. Thus, in our bilateral preconditioning technique, we choose the (P)CG method based Gohberg-Semencul formula (GSF) [52] for fast solving Eq. (2.3). However, the GSF formula cannot be applied to solve block Toeplitz systems with Toeplitz blocks. Thus, for solving the two-dimensional problem of Eq. (1.1), we have to make a small change in the bilateral preconditioning technique. That is, we use the (P)CG method to solve the two-dimensional version of (2.3). Moreover, in this paper, we construct a  $\tau$ -preconditioner for (2.3), see [51] for details.*

**Example 1.** We consider Eq. (1.1) with  $x_L = 0$ ,  $\kappa = x_R = T = 1$  and the source term

$$f(x, t) = \left( \frac{\Gamma(4 + \alpha)}{\Gamma(4)} t^3 + \frac{\Gamma(3)}{\Gamma(3 - \alpha)} t^{2 - \alpha} \right) x^2 (1 - x)^2 + \frac{\kappa (t^{3 + \alpha} + t^2 + 1)}{2 \cos(\pi\beta/2)} \times$$

$$\left\{ \frac{\Gamma(3)}{\Gamma(3 - \beta)} [x^{2 - \beta} + (1 - x)^{2 - \beta}] - \frac{2\Gamma(4)}{\Gamma(4 - \beta)} [x^{3 - \beta} + (1 - x)^{3 - \beta}] + \right.$$

$$\left. \frac{\Gamma(5)}{\Gamma(5 - \beta)} [x^{4 - \beta} + (1 - x)^{4 - \beta}] \right\}.$$

The exact solution is  $u(x, t) = (t^{3 + \alpha} + t^2 + 1) x^2 (1 - x)^2$ .

Table 1 lists the errors and the observed time convergence orders for different values of  $\alpha$  and  $\beta$ . From

Table 1: Numerical errors and the observed time convergence orders for Example 1 with  $N = M^{(3-\alpha)/2}$ .

$(\alpha, \beta)$	$M$	$Err_\infty(h, \tau)$	$CO_{\infty, \tau}$	$Err_2(h, \tau)$	$CO_{2, \tau}$
(0.1, 1.5)	10	3.3558E-04	–	2.1958E-04	–
	20	4.2391E-05	2.9848	2.7415E-05	3.0017
	40	5.3517E-06	2.9857	3.5198E-06	2.9614
	80	6.7403E-07	2.9891	4.5958E-07	2.9371
	160	9.2695E-08	2.8622	6.0949E-08	2.9146
(0.4, 1.7)	10	1.0146E-03	–	6.9999E-04	–
	20	1.5215E-04	2.7373	1.0266E-04	2.7695
	40	2.4455E-05	2.6373	1.6239E-05	2.6603
	80	3.8098E-06	2.6823	2.5054E-06	2.6963
	160	5.9581E-07	2.6768	3.9086E-07	2.6803
(0.7, 1.4)	10	1.2174E-03	–	8.0414E-04	–
	20	2.4993E-04	2.2842	1.6106E-04	2.3198
	40	4.9078E-05	2.3484	3.1689E-05	2.3455
	80	9.5109E-06	2.3674	6.2572E-06	2.3404
	160	1.8604E-06	2.3540	1.2594E-06	2.3128
(0.9, 1.9)	10	4.0154E-03	–	2.8992E-03	–
	20	9.8220E-04	2.0315	7.0490E-04	2.0402
	40	2.3079E-04	2.0894	1.6464E-04	2.0981
	80	5.4304E-05	2.0875	3.8477E-05	2.0972
	160	1.2432E-05	2.1270	8.7530E-06	2.1361

this table, we can see that for fixed  $N = M^{(3-\alpha)/2}$ , the observed convergence order in time is  $3 - \alpha$ . Table 2 reports the errors and the observed convergence order in space for different values of  $\alpha$  and  $\beta$ . It shows that for fixed  $M = 1024$ , the errors in Table 2 decrease steadily with increasing  $N$ , and the observed convergence order in space is 2 as expected. In a word, our method is reliable and accurate.

**Example 2.** Consider Eq. (1.1) with  $\kappa = T = 1$ ,  $x_L = -1$ ,  $x_R = 1$  and the source term

$$f(x, t) = \frac{\Gamma(4 + \alpha)}{\Gamma(4)} t^3 (1 + x)^2 (1 - x)^2 + \frac{\kappa (t^{3+\alpha} + 1)}{2 \cos(\pi\beta/2)} \left\{ \frac{4 \Gamma(3)}{\Gamma(3 - \beta)} [(1 + x)^{2-\beta} + (1 - x)^{2-\beta}] - \frac{4 \Gamma(4)}{\Gamma(4 - \beta)} [(1 + x)^{3-\beta} + (1 - x)^{3-\beta}] + \frac{\Gamma(5)}{\Gamma(5 - \beta)} [(1 + x)^{4-\beta} + (1 - x)^{4-\beta}] \right\}.$$

The exact solution is  $u(x, t) = (t^{3+\alpha} + 1) (1 + x)^2 (1 - x)^2$ .

Table 3 lists the performances of methods BS, BFSM,  $\mathcal{I}$  and  $\mathcal{P}$ . In this table and the following tables, “OoM” means out of memory, “†” represents that the (P)BiCGSTAB/(P)CG method does not converge to the desired tolerance within 1000 iterations. Compared with the method BS, our method  $\mathcal{P}$  indeed accelerates solving Eq. (2.6) and reduces the storage requirement. Compared with the method BFSM, for large  $M$  and  $N$  (i.e.,  $M = N = 1024, 2048$ ), the CPU time of the method  $\mathcal{P}$  is smaller. For the unsatisfied cases (i.e.,  $M = N = 128, 256, 512$ ), although the numbers Time of the method  $\mathcal{P}$  are larger than the BFSM method, the method  $\mathcal{P}$  still has two advantages in terms of storage requirement and parallel computing. Moreover, we notice that the numbers Iter1 and Iter2 of the method  $\mathcal{P}$  are slightly influenced by the mesh

Table 2: Numerical errors and the observed space convergence orders for Example 1 with  $M = 1024$ .

$(\alpha, \beta)$	$N$	$Err_\infty(h, \tau)$	$CO_{\infty, \tau}$	$Err_2(h, \tau)$	$CO_{2, \tau}$
(0.1, 1.5)	10	3.1533E-03	–	2.1393E-03	–
	20	7.3035E-04	2.1102	4.8195E-04	2.1502
	40	1.7021E-04	2.1013	1.1044E-04	2.1256
	80	3.9928E-05	2.0918	2.5825E-05	2.0964
	160	9.4280E-06	2.0824	6.1603E-06	2.0677
(0.4, 1.7)	10	4.1944E-03	–	2.9495E-03	–
	20	9.9378E-04	2.0775	6.8541E-04	2.1054
	40	2.3585E-04	2.0751	1.5982E-04	2.1005
	80	5.6098E-05	2.0718	3.7467E-05	2.0928
	160	1.3377E-05	2.0682	8.8415E-06	2.0833
(0.7, 1.4)	10	2.4866E-03	–	1.6468E-03	–
	20	5.7380E-04	2.1156	3.7013E-04	2.1536
	40	1.3363E-04	2.1023	8.5825E-05	2.1086
	80	3.1405E-05	2.0892	2.0534E-05	2.0634
	160	7.4461E-06	2.0764	5.0382E-06	2.0270
(0.9, 1.9)	10	5.4166E-03	–	3.9271E-03	–
	20	1.3277E-03	2.0285	9.5644E-04	2.0377
	40	3.2529E-04	2.0291	2.3276E-04	2.0388
	80	7.9708E-05	2.0289	5.6655E-05	2.0386
	160	1.9545E-05	2.0279	1.3802E-05	2.0373

size. It should be mentioning that from Table 3, for  $\alpha = 0.9 (> 0.3624)$ , our method  $\mathcal{P}$  still performs well.

Table 4: The condition numbers of  $\tilde{\mathcal{M}}$  and  $P_l^{-1}\tilde{\mathcal{M}}P_r^{-1}$  for  $M = N$  for Example 2.

$(\alpha, \beta)$	$N$	$\kappa_2(\tilde{\mathcal{M}})$	$\kappa_2(P_l^{-1}\tilde{\mathcal{M}}P_r^{-1})$
(0.1, 1.1)	16	9.86	1.23
	32	20.63	1.30
	64	43.64	1.36
	128	92.89	1.42
(0.2, 1.7)	16	38.04	1.12
	32	123.25	1.15
	64	400.27	1.18
	128	1300.85	1.21
(0.35, 1.5)	16	25.02	1.17
	32	68.98	1.22
	64	192.69	1.27
	128	541.93	1.31
(0.9, 1.9)	16	70.45	1.04
	32	243.78	1.06
	64	870.27	1.07
	128	3171.08	1.08

Table 4 lists the condition numbers of  $\tilde{\mathcal{M}}$  and  $P_l^{-1}\tilde{\mathcal{M}}P_r^{-1}$  for different values of  $\alpha$  and  $\beta$ . From this table, we see that  $\kappa_2(P_l^{-1}\tilde{\mathcal{M}}P_r^{-1}) < 2\sqrt{3}$  for  $\alpha < 0.3624$ . This is in good agreement with our theoretical analysis in Section 3.2. Although we fail to give the bound of  $\kappa_2(P_l^{-1}\tilde{\mathcal{M}}P_r^{-1})$  for  $\alpha > 0.3624$  theoretically, Table 4 shows that for  $\alpha = 0.9 (> 0.3624)$ , the condition number of  $P_l^{-1}\tilde{\mathcal{M}}P_r^{-1}$  is still less than  $2\sqrt{3}$ . Fig. 2

Table 3: Results of various methods for  $M = N$  for Example 2.

$(\alpha, \beta)$	$N$	BS	BFSM	$\mathcal{I}$		$\mathcal{P}$	
		Time	Time	(Iter1, Iter2)	Time	(Iter1, Iter2)	Time
(0.1, 1.1)	128	6.268	0.111	(56.0, 61.0)	1.021	(7.0, 5.0)	0.537
	256	1160.576	0.524	(80.0, 89.0)	5.141	(7.0, 5.0)	1.831
	512	> 5 hours	5.097	(114.0, 137.0)	29.161	(8.0, 5.0)	5.985
	1024	OoM	50.948	(162.0, 191.0)	261.795	(8.0, 5.0)	20.847
	2048	OoM	537.730	(228.0, 283.0)	1605.622	(8.0, 6.0)	89.736
(0.2, 1.7)	128	6.220	0.116	(113.0, 233.0)	7.692	(6.0, 4.0)	0.447
	256	1092.552	0.534	(202.0, 438.0)	48.579	(6.0, 5.0)	1.873
	512	> 5 hours	5.057	(360.0, 829.0)	307.938	(6.0, 5.0)	5.786
	1024	OoM	48.755	†	†	(6.0, 5.0)	20.128
	2048	OoM	537.980	†	†	(7.0, 6.0)	86.305
(0.35, 1.5)	128	6.210	0.110	(78.0, 189.0)	6.426	(6.0, 5.0)	0.539
	256	1277.143	0.526	(116.0, 310.0)	34.513	(6.0, 5.0)	1.835
	512	> 5 hours	4.963	(163.0, 569.0)	212.494	(6.0, 5.0)	5.789
	1024	OoM	51.936	†	†	(6.0, 5.0)	20.159
	2048	OoM	582.579	†	†	(6.0, 6.0)	86.159
(0.9, 1.9)	128	6.211	0.127	†	†	(3.0, 4.0)	0.459
	256	1805.931	0.604	†	†	(3.0, 4.0)	1.534
	512	> 5 hours	5.588	†	†	(3.0, 4.0)	4.831
	1024	OoM	52.250	†	†	(3.0, 4.0)	16.527
	2048	OoM	599.093	†	†	(3.0, 4.0)	60.787

shows the spectrum of  $\tilde{\mathcal{M}}$ ,  $P_l^{-1}\tilde{\mathcal{M}}$ ,  $\tilde{\mathcal{M}}P_r^{-1}$  and  $P_l^{-1}\tilde{\mathcal{M}}P_r^{-1}$ . From this figure, the eigenvalues of  $P_l^{-1}\tilde{\mathcal{M}}P_r^{-1}$  are more clustered around 1 than  $P_l^{-1}\tilde{\mathcal{M}}$  and  $\tilde{\mathcal{M}}P_r^{-1}$ . In a word, Table 3 and Fig. 2 indicate that our preconditioning technique is reliable and efficient for solving Eq. (1.1).

**Example 3.** In this example, we extend our bilateral preconditioning technique to solve the following two-dimensional problem of Eq. (1.1):

$$\begin{cases} {}_0^C \mathcal{D}_t^\alpha u(x, y, t) = 0.5 \left( \frac{\partial^\beta u(x, y, t)}{\partial |x|^\beta} + \frac{\partial^\beta u(x, y, t)}{\partial |y|^\beta} \right) + f(x, y, t), & (x, y) \in \Omega, t \in (0, 1], \\ u(x, y, t) = 0, & (x, y) \in \partial\Omega, t \in [0, 1], \\ u(x, y, 0) = \phi(x, y), & (x, y) \in \Omega, \end{cases}$$

where  $\Omega = (0, 1)^2$ ,  $\partial\Omega$  is the boundary of  $\Omega$ ,  $\phi(x, y) = 200x^2(1-x)^2y^2(1-y)^2$  and

$$\begin{aligned} f(x, y, t) = & \frac{200\Gamma(3+\alpha+\beta)}{\Gamma(3+\beta)} t^{2+\beta} x^2(1-x)^2 y^2(1-y)^2 + \frac{50(t^{2+\alpha+\beta}+1)}{\cos(\pi\beta/2)} \times \\ & \left\{ \frac{\Gamma(3)}{\Gamma(3-\beta)} [x^{2-\beta} + (1-x)^{2-\beta}] - \frac{2\Gamma(4)}{\Gamma(4-\beta)} [x^{3-\beta} + (1-x)^{3-\beta}] + \right. \\ & \left. \frac{\Gamma(5)}{\Gamma(5-\beta)} [x^{4-\beta} + (1-x)^{4-\beta}] \right\} y^2(1-y)^2 + \frac{50(t^{2+\alpha+\beta}+1)}{\cos(\pi\beta/2)} \times \\ & \left\{ \frac{\Gamma(3)}{\Gamma(3-\beta)} [y^{2-\beta} + (1-y)^{2-\beta}] - \frac{2\Gamma(4)}{\Gamma(4-\beta)} [y^{3-\beta} + (1-y)^{3-\beta}] + \right. \end{aligned}$$

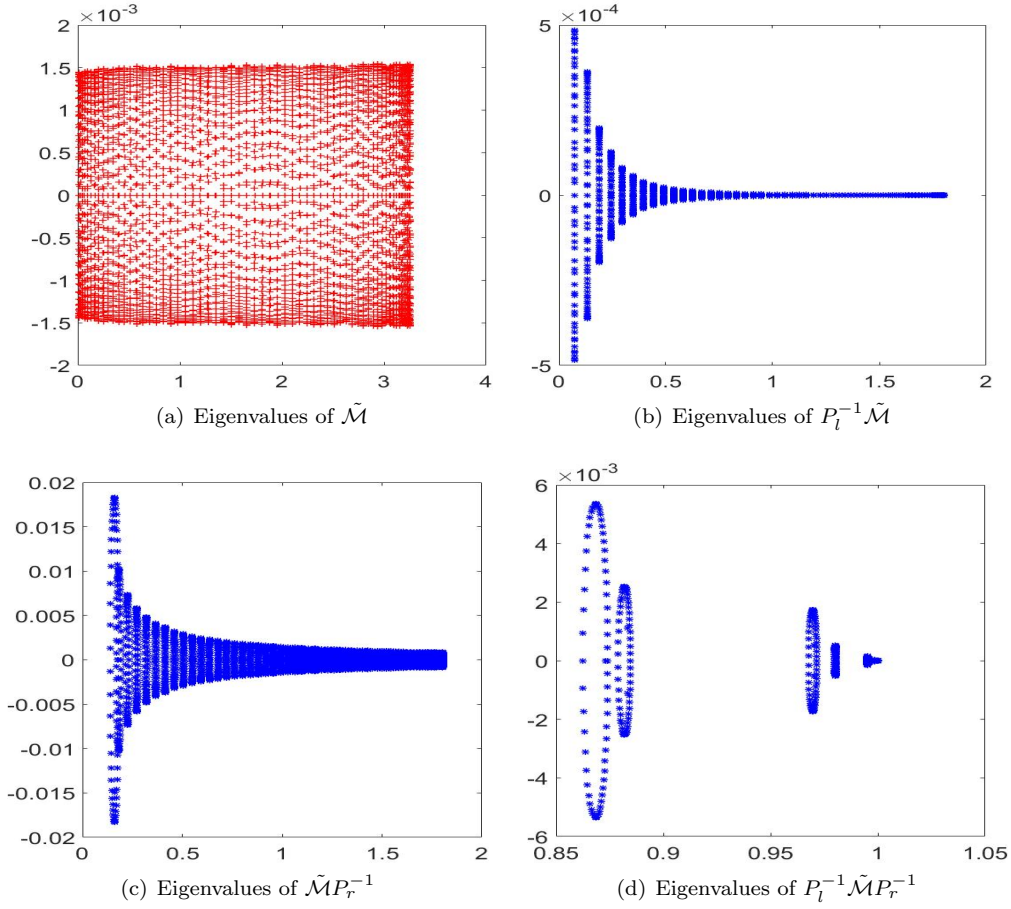


Fig. 2: Spectrum of  $\tilde{\mathcal{M}}$ ,  $P_l^{-1}\tilde{\mathcal{M}}$ ,  $\tilde{\mathcal{M}}P_r^{-1}$  and  $P_l^{-1}\tilde{\mathcal{M}}P_r^{-1}$  for  $(\alpha, \beta) = (0.2, 1.7)$  and  $M = N = 64$  for Example 2.

$$\frac{\Gamma(5)}{\Gamma(5-\beta)} [y^{4-\beta} + (1-y)^{4-\beta}] \} x^2(1-x)^2.$$

The exact solution is  $u(x, y, t) = 200 (t^{2+\alpha+\beta} + 1) x^2(1-x)^2 y^2(1-y)^2$ .

Let  $N_x$  and  $N_y$  be the number of grid points in  $x$ - and  $y$ -direction, respectively. In this example, we fix  $N_x = N_y = N$ . Table 5 lists the results of various methods (i.e., BS, BFSM,  $\mathcal{I}$  and  $\mathcal{P}$ ) for different values of  $\alpha$  and  $\beta$ . This table indicates that the proposed method greatly reduces the storage requirement and CPU time. For large  $N$ , that is  $N = 32, 64, 128, 256$ , the numbers Time of the method  $\mathcal{P}$  are smaller than the method BFSM. It is worth mentioning that the number of iterations (i.e., Iter1 and Iter2) required by the method  $\mathcal{P}$  is slightly dependent on the mesh size. From Table 6, we can see that the condition number of  $P_l^{-1}\tilde{\mathcal{M}}P_r^{-1}$  is less than  $2\sqrt{3}$ , even for  $\alpha = 0.9 (> 0.3624)$ . The spectrum of  $\tilde{\mathcal{M}}$ ,  $P_l^{-1}\tilde{\mathcal{M}}$ ,  $\tilde{\mathcal{M}}P_r^{-1}$  and  $P_l^{-1}\tilde{\mathcal{M}}P_r^{-1}$  for  $(\alpha, \beta) = (0.9, 1.9)$  are drawn in Fig. 3. From this figure, the eigenvalues of  $P_l^{-1}\tilde{\mathcal{M}}$ ,  $\tilde{\mathcal{M}}P_r^{-1}$  and  $P_l^{-1}\tilde{\mathcal{M}}P_r^{-1}$  are all clustered around 1. The eigenvalues of  $P_l^{-1}\tilde{\mathcal{M}}P_r^{-1}$  are the most clustered one among them. Moreover, Fig. 4 compares the exact solution and numerical solution for  $(\alpha, \beta) = (0.35, 1.5)$ . It

indicates that our numerical method in Section 2.1 is accurate.

Table 5: Results of various methods for  $M = N$  for Example 3.

$(\alpha, \beta)$	$N$	BS	BFSM	$\mathcal{I}$		$\mathcal{P}$	
		Time	Time	(Iter1, Iter2)	Time	(Iter1, Iter2)	Time
(0.1, 1.1)	16	15.838	0.075	(18.0, 19.0)	0.584	(6.0, 4.0)	0.202
	32	> 5 hours	1.789	(27.0, 33.0)	2.333	(7.0, 5.0)	1.014
	64	> 5 hours	114.623	(42.0, 51.0)	18.085	(7.0, 5.0)	5.264
	128	> 5 hours	$\approx 3.7$ hours	(62.0, 69.0)	205.295	(8.0, 5.0)	38.762
	256	OoM	> 5 hours	(91.0, 92.0)	1913.149	(9.0, 5.0)	358.067
(0.2, 1.7)	16	16.083	0.084	(25.0, 36.0)	0.524	(5.0, 4.0)	0.182
	32	> 5 hours	1.809	(47.0, 72.0)	5.101	(6.0, 4.0)	0.798
	64	> 5 hours	111.289	(85.0, 125.0)	45.596	(6.0, 4.0)	4.339
	128	> 5 hours	$\approx 3.7$ hours	(154.0, 293.0)	860.445	(7.0, 4.0)	31.485
	256	OoM	> 5 hours	(278.0, 544.0)	$\approx 3.1$ hours	(7.0, 5.0)	354.081
(0.35, 1.5)	16	15.783	0.060	(22.0, 40.0)	0.574	(5.0, 4.0)	0.187
	32	> 5 hours	1.811	(37.0, 64.0)	4.718	(6.0, 5.0)	0.997
	64	> 5 hours	110.938	(60.0, 108.0)	39.431	(7.0, 5.0)	5.282
	128	> 5 hours	$\approx 3.7$ hours	(97.0, 186.0)	549.375	(7.0, 5.0)	39.452
	256	OoM	> 5 hours	(154.0, 333.0)	6901.452	(8.0, 5.0)	359.428
(0.9, 1.9)	16	15.910	0.075	(18.0, 72.0)	1.073	(4.0, 3.0)	0.173
	32	> 5 hours	1.910	(22.0, 202.0)	13.323	(4.0, 3.0)	0.740
	64	> 5 hours	112.491	(22.0, 644.0)	229.510	(4.0, 4.0)	4.962
	128	> 5 hours	$\approx 3.7$ hours	†	†	(3.0, 4.0)	36.029
	256	OoM	> 5 hours	†	†	(3.0, 4.0)	323.964

Table 6: The condition numbers of  $\tilde{\mathcal{M}}$  and  $P_l^{-1}\tilde{\mathcal{M}}P_r^{-1}$  for  $M = N$  for Example 3.

$(\alpha, \beta)$	$N$	$\kappa_2(\tilde{\mathcal{M}})$	$\kappa_2(P_l^{-1}\tilde{\mathcal{M}}P_r^{-1})$
(0.1, 1.1)	8	5.83	1.20
	16	12.50	1.28
	32	26.71	1.36
(0.2, 1.7)	8	26.71	1.36
	16	49.93	1.14
	32	163.39	1.18
(0.35, 1.5)	8	11.40	1.15
	16	32.43	1.21
	32	91.73	1.27
(0.9, 1.9)	8	22.78	1.04
	16	22.78	1.04
	32	306.82	1.07

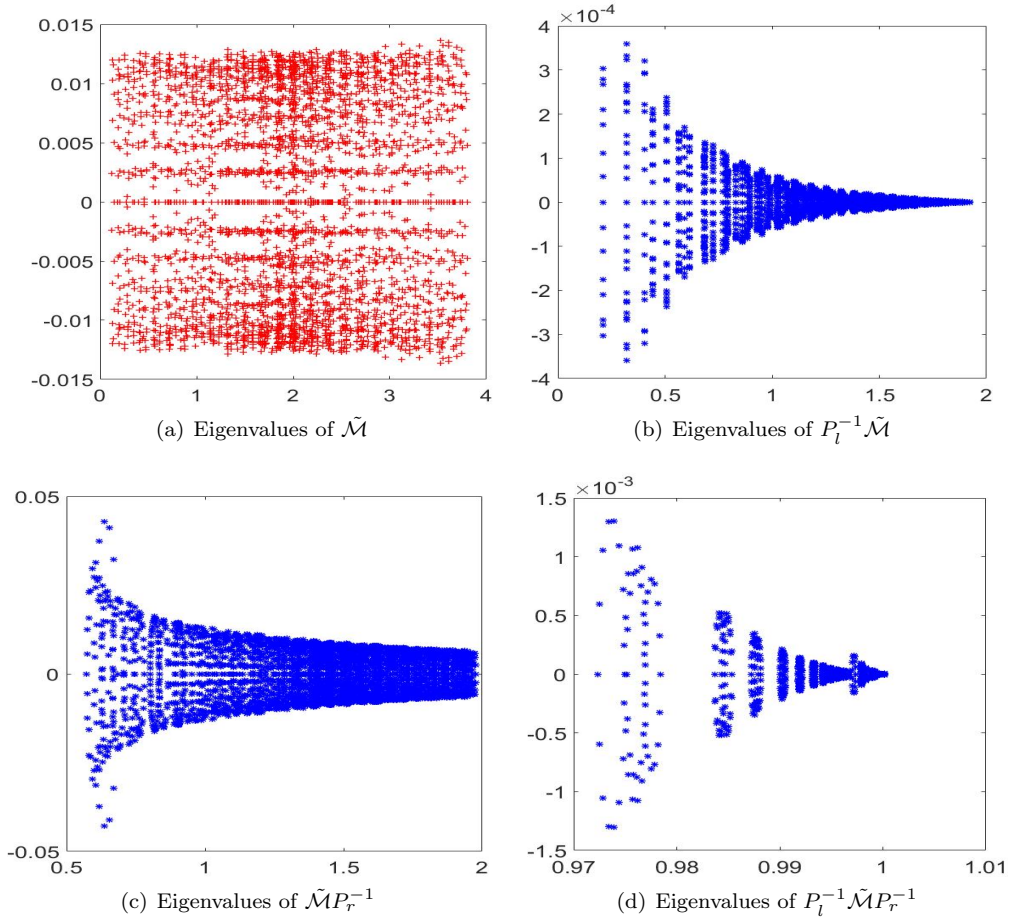


Fig. 3: Spectrum of  $\tilde{\mathcal{M}}$ ,  $P_l^{-1}\tilde{\mathcal{M}}$ ,  $\tilde{\mathcal{M}}P_r^{-1}$  and  $P_l^{-1}\tilde{\mathcal{M}}P_r^{-1}$  for  $(\alpha, \beta) = (0.9, 1.9)$  and  $M = N = 16$  for Example 3.

## 5. Concluding remarks

In this article, we propose a bilateral preconditioning technique to solve the L2-type all-at-once system (2.6) arising from the TSFBTE (1.1). Firstly, combining the L2-type formula [45] and the fractional centered difference method [46, 47], we propose and analyse an L2-type difference scheme (2.2) with  $3 - \alpha$  accuracy in time to approximate Eq. (1.1). Secondly, we derive the L2-type all-at-once system (2.6) based on this scheme. In order to obtain the solution of Eq. (2.6) efficiently, the left ( $P_l$ ) and right ( $P_r$ ) preconditioners are designed. The condition number of the preconditioned matrix  $P_l^{-1}\tilde{\mathcal{M}}P_r^{-1}$  is analyzed. Finally, numerical examples are reported to show the performance of our method. Moreover, in Example 3, we extend our bilateral preconditioning technique to solve the two-dimensional problem of Eq. (1.1). It is worth mentioning that our method can be extended to solve linear all-at-once systems with graded time steps such as [43]. In our future work, we will use the proposed preconditioning technique to solve semilinear problems, e.g., the

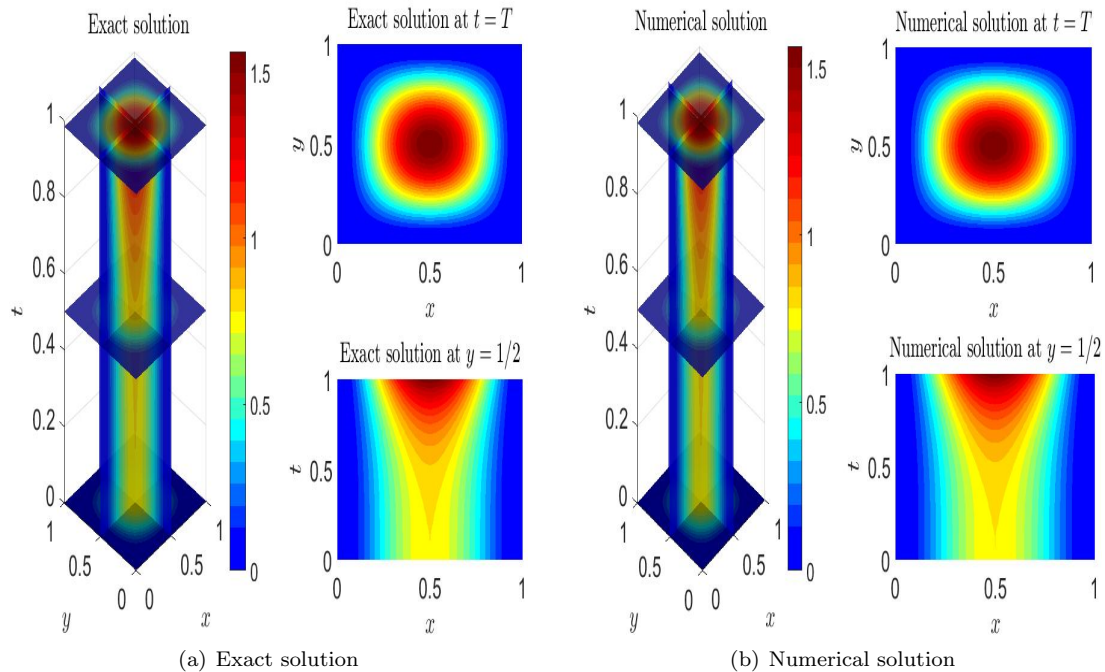


Fig. 4: Comparison of exact solution and numerical solution for  $(\alpha, \beta) = (0.35, 1.5)$  and  $M = N = 64$  for Example 3.

Volterra Allen-Cahn equation with weakly singular kernel [19].

## Acknowledgments

*This research is supported by the National Natural Science Foundation of China (Nos. 11801463 and 12101089), the Applied Basic Research Project of Sichuan Province (No. 2020YJ0007), the Natural Science Foundation of Sichuan Province (Nos. 2022NSFSC1815 and 2023NSFSC1326) and the Sichuan Science and Technology Program (No. 2022ZYD0006).*

## References

### References

- [1] E. Lenzi, P. Fernandes, T. Petrucci, H. Mukai, H. Ribeiro, Anomalous-diffusion approach applied to the electrical response of water, *Phys. Rev. E* 84 (2011) 041128. doi:10.1103/PhysRevE.84.041128.
- [2] H. Sun, Y. Zhang, D. Baleanu, W. Chen, Y. Chen, A new collection of real world applications of fractional calculus in science and engineering, *Commun. Nonlinear Sci. Numer. Simul.* 64 (2018) 213–231.
- [3] Y. Zhang, H. Sun, H. H. Stowell, M. Zayernouri, S. E. Hansen, A review of applications of fractional calculus in earth system dynamics, *Chaos, Solitons & Fractals* 102 (2017) 29–46.
- [4] M. Ghazal, M. Behrouz, Modelling solute transport in homogeneous and heterogeneous porous media using spatial fractional advection-dispersion equation, *Soil Water Res.* 13 (2018) 18–28.

- [5] Y.-F. Pu, J.-L. Zhou, X. Yuan, Fractional differential mask: a fractional differential-based approach for multiscale texture enhancement, *IEEE Trans. Image Process.* 19 (2009) 491–511.
- [6] L. Guo, X.-L. Zhao, X.-M. Gu, Y.-L. Zhao, Y.-B. Zheng, T.-Z. Huang, Three-dimensional fractional total variation regularized tensor optimized model for image deblurring, *Appl. Math. Comput.* 404 (2021) 126224. doi:10.1016/j.amc.2021.126224.
- [7] R. Metzler, J. Klafter, The random walk’s guide to anomalous diffusion: a fractional dynamics approach, *Phys. Rep.* 339 (2000) 1–77.
- [8] R. Metzler, J. Klafter, The restaurant at the end of the random walk: recent developments in the description of anomalous transport by fractional dynamics, *J. Phys. A: Math. Gen.* 37 (2004) R161. doi:10.1088/0305-4470/37/31/r01.
- [9] B. Henry, T. Langlands, S. Wearne, Anomalous diffusion with linear reaction dynamics: from continuous time random walks to fractional reaction-diffusion equations, *Phys. Rev. E* 74 (2006) 031116. doi:10.1103/PhysRevE.74.031116.
- [10] G. Chi, G. Li, C. Sun, X. Jia, Numerical solution to the space-time fractional diffusion equation and inversion for the space-dependent diffusion coefficient, *J. Comput. Theor. Transp.* 46 (2) (2017) 122–146.
- [11] Q. Yu, F. Liu, I. Turner, K. Burrage, Stability and convergence of an implicit numerical method for the space and time fractional Bloch-Torrey equation, *Phil. Trans. R. Soc. A* 371 (2013) 20120150. doi:10.1098/rsta.2012.0150.
- [12] Y. Zhu, Z.-Z. Sun, A high-order difference scheme for the space and time fractional Bloch-Torrey equation, *Comput. Methods Appl. Math.* 18 (2018) 147–164.
- [13] I. Podlubny, A. Chechkin, T. Skovranek, Y. Chen, B. M. V. Jara, Matrix approach to discrete fractional calculus II: partial fractional differential equations, *J. Comput. Phys.* 228 (2009) 3137–3153.
- [14] R. L. Magin, O. Abdullah, D. Baleanu, X. J. Zhou, Anomalous diffusion expressed through fractional order differential operators in the Bloch-Torrey equation, *J. Magn. Reson.* 190 (2008) 255–270.
- [15] Q. Yu, F. Liu, I. Turner, K. Burrage, Numerical investigation of three types of space and time fractional Bloch-Torrey equations in 2D, *Cent. Eur. J. Phys.* 11 (2013) 646–665.
- [16] M. Li, X.-M. Gu, C. Huang, M. Fei, G. Zhang, A fast linearized conservative finite element method for the strongly coupled nonlinear fractional Schrödinger equations, *J. Comput. Phys.* 358 (2018) 256–282.
- [17] S. Duo, H. W. van Wyk, Y. Zhang, A novel and accurate finite difference method for the fractional Laplacian and the fractional Poisson problem, *J. Comput. Phys.* 355 (2018) 233–252.
- [18] H.-L. Liao, W. McLean, J. Zhang, A discrete Grönwall inequality with applications to numerical schemes for subdiffusion problems, *SIAM J. Numer. Anal.* 57 (2019) 218–237.
- [19] X.-M. Gu, S.-L. Wu, A parallel-in-time iterative algorithm for Volterra partial integro-differential problems with weakly singular kernel, *J. Comput. Phys.* 417 (2020) 109576. doi:10.1016/j.jcp.2020.109576.
- [20] J. Shen, C. Li, Z.-Z. Sun, An H2N2 interpolation for Caputo derivative with order in (1,2) and its application to time-fractional wave equations in more than one space dimension, *J. Sci. Comput.* 83 (2020) 38. doi:10.1007/s10915-020-01219-8.
- [21] Y.-L. Zhao, M. Li, A. Ostermann, X.-M. Gu, An efficient second-order energy stable BDF scheme for the space fractional Cahn-Hilliard equation, *BIT* 61 (2021) 1061–1092.
- [22] W.-H. Luo, X.-M. Gu, L. Yang, J. Meng, A Lagrange-quadratic spline optimal collocation method for the time tempered fractional diffusion equation, *Math. Comput. Simul.* 182 (2021) 1–24.
- [23] D. Nie, J. Sun, W. Deng, Numerical algorithm for the space-time fractional Fokker-Planck system with two internal states, *Numer. Math.* 146 (2020) 481–511.
- [24] H. Chen, C. Sheng, L.-L. Wang, On explicit form of the FEM stiffness matrix for the integral fractional Laplacian on non-uniform meshes, *Appl. Math. Lett.* 113 (2021) 106864. doi:10.1016/j.aml.2020.106864.
- [25] Q. Zhang, L. Zhang, H.-W. Sun, A three-level finite difference method with preconditioning technique for two-dimensional

- nonlinear fractional complex Ginzburg-Landau equations, *J. Comput. Appl. Math.* 389 (2021) 113355. doi:10.1016/j.cam.2020.113355.
- [26] Q. Yang, I. Turner, F. Liu, M. Ilić, Novel numerical methods for solving the time-space fractional diffusion equation in two dimensions, *SIAM J. Sci. Comput.* 33 (2011) 1159–1180.
- [27] H. Sun, Z.-Z. Sun, G.-H. Gao, Some high order difference schemes for the space and time fractional Bloch-Torrey equations, *Appl. Math. Comput.* 281 (2016) 356–380.
- [28] S. Arshad, J. Huang, A. Q. Khaliq, Y. Tang, Trapezoidal scheme for time-space fractional diffusion equation with Riesz derivative, *J. Comput. Phys.* 350 (2017) 1–15.
- [29] W. Bu, Y. Tang, Y. Wu, J. Yang, Finite difference/finite element method for two-dimensional space and time fractional Bloch–Torrey equations, *J. Comput. Phys.* 293 (2015) 264–279.
- [30] M. Dehghan, M. Abbaszadeh, An efficient technique based on finite difference/finite element method for solution of two-dimensional space/multi-time fractional Bloch-Torrey equations, *Appl. Numer. Math.* 131 (2018) 190–206.
- [31] D. Wang, J. Zou, Dissipativity and contractivity analysis for fractional functional differential equations and their numerical approximations, *SIAM J. Numer. Anal.* 57 (2019) 1445–1470.
- [32] S. Zhai, Z. Weng, X. Feng, J. Yuan, Investigations on several high-order ADI methods for time-space fractional diffusion equation, *Numer. Algorithms* 82 (2019) 69–106.
- [33] Y.-C. Huang, S.-L. Lei, Fast solvers for finite difference scheme of two-dimensional time-space fractional differential equations, *Numer. Algorithms* 84 (2020) 37–62.
- [34] N. Wang, M. Fei, C. Huang, G. Zhang, M. Li, Dissipation-preserving Galerkin-Legendre spectral methods for two-dimensional fractional nonlinear wave equations, *Comput. Math. Appl.* 80 (2020) 617–635.
- [35] X.-M. Gu, H.-W. Sun, Y.-L. Zhao, X. Zheng, An implicit difference scheme for time-fractional diffusion equations with a time-invariant type variable order, *Appl. Math. Lett.* 120 (2021) 107270. doi:10.1016/j.aml.2021.107270.
- [36] X. Yue, K. Pan, J. Zhou, Z. Weng, S. Shu, J. Tang, A multigrid-reduction-in-time solver with a new two-level convergence for unsteady fractional Laplacian problems, *Comput. Math. Appl.* 89 (2021) 57–67.
- [37] X. Lu, H.-K. Pang, H.-W. Sun, Fast approximate inversion of a block triangular Toeplitz matrix with applications to fractional sub-diffusion equations, *Numer. Linear Algebra Appl.* 22 (2015) 866–882.
- [38] R. Ke, M. K. Ng, H.-W. Sun, A fast direct method for block triangular Toeplitz-like with tri-diagonal block systems from time-fractional partial differential equations, *J. Comput. Phys.* 303 (2015) 203–211.
- [39] Y.-C. Huang, S.-L. Lei, A fast numerical method for block lower triangular Toeplitz with dense Toeplitz blocks system with applications to time-space fractional diffusion equations, *Numer. Algorithms* 76 (2017) 605–616.
- [40] D. Bertaccini, F. Durastante, Limited memory block preconditioners for fast solution of fractional partial differential equations, *J. Sci. Comput.* 77 (2018) 950–970.
- [41] X.-L. Lin, M. K. Ng, A fast solver for multidimensional time-space fractional diffusion equation with variable coefficients, *Comput. Math. Appl.* 78 (2019) 1477–1489.
- [42] Y.-L. Zhao, P.-Y. Zhu, X.-M. Gu, X.-L. Zhao, H.-Y. Jian, A preconditioning technique for all-at-once system from the nonlinear tempered fractional diffusion equation, *J. Sci. Comput.* 83 (2020) 10. doi:10.1007/s10915-020-01193-1.
- [43] Y.-L. Zhao, X.-M. Gu, A. Ostermann, A preconditioning technique for an all-at-once system from Volterra subdiffusion equations with graded time steps, *J. Sci. Comput.* 88 (2021) 11. doi:10.1007/s10915-021-01527-7.
- [44] X.-L. Lin, M. K. Ng, Y. Zhi, A parallel-in-time two-sided preconditioning for all-at-once system from a non-local evolutionary equation with weakly singular kernel, *J. Comput. Phys.* 434 (2021) 110221. doi:10.1016/j.jcp.2021.110221.
- [45] A. A. Alikhanov, C. Huang, A high-order L2 type difference scheme for the time-fractional diffusion equation, *Appl. Math. Comput.* 411 (2021) 126545. doi:10.1016/j.amc.2021.126545.
- [46] C. Çelik, M. Duman, Crank-Nicolson method for the fractional diffusion equation with the Riesz fractional derivative, *J.*

- Comput. Phys. 231 (2012) 1743–1750.
- [47] L. Zhang, Q. Zhang, H.-W. Sun, Exponential Runge-Kutta method for two-dimensional nonlinear fractional complex Ginzburg–Landau equations, *J. Sci. Comput.* 83 (2020) 1–24.
- [48] S. Jiang, J. Zhang, Q. Zhang, Z. Zhang, Fast evaluation of the Caputo fractional derivative and its applications to fractional diffusion equations, *Commun. Comput. Phys.* 21 (2017) 650–678.
- [49] X.-M. Gu, H.-W. Sun, Y. Zhang, Y.-L. Zhao, Fast implicit difference schemes for time-space fractional diffusion equations with the integral fractional Laplacian, *Math. Meth. Appl. Sci.* 44 (2021) 441–463.
- [50] J. E. Macías-Díaz, A structure-preserving method for a class of nonlinear dissipative wave equations with Riesz space-fractional derivatives, *J. Comput. Phys.* 351 (2017) 40–58.
- [51] D. Bini, F. Benedetto, A new preconditioner for the parallel solution of positive definite Toeplitz systems, in: *Proceedings of the Second Annual ACM Symposium on Parallel Algorithms and Architectures*, New York, 1990, pp. 220–223. doi: 10.1145/97444.97688.
- [52] M. K. Ng, *Iterative Methods for Toeplitz Systems*, Oxford University Press, New York, NY, 2004.
- [53] Y. Saad, *Iterative Methods for Sparse Linear Systems*, 2nd ed., SIAM, Philadelphia, PA, 2003.
- [54] H. A. Van der Vorst, Bi-CGSTAB: A fast and smoothly converging variant of Bi-CG for the solution of nonsymmetric linear systems, *SIAM J. Sci. Stat. Comput.* 13 (1992) 631–644.
- [55] D. Commenges, M. Monsion, Fast inversion of triangular Toeplitz matrices, *IEEE Trans. Autom. Control* 29 (1984) 250–251.
- [56] F.-R. Lin, W.-K. Ching, M. K. Ng, Fast inversion of triangular Toeplitz matrices, *Theor. Comput. Sci.* 315 (2004) 511–523.
- [57] G.-H. Gao, Z.-Z. Sun, H.-W. Zhang, A new fractional numerical differentiation formula to approximate the Caputo fractional derivative and its applications, *J. Comput. Phys.* 259 (2014) 33–50.
- [58] R. S. Varga, *Geršgorin and His Circles*, Springer-Verlag, Berlin, 2004.
- [59] X. Huang, X.-L. Lin, M. K. Ng, H.-W. Sun, Spectral analysis for preconditioning of multi-dimensional Riesz fractional diffusion equations, arXiv preprint arXiv:2102.01371 (2021) 22 pages.
- [60] R. A. Horn, C. R. Johnson, *Matrix Analysis*, Cambridge University Press, Cambridge, 2012.